ACCEPTED FROM OPEN CALL

Ambient Noise in Warm Shallow Waters: A Communications Perspective

Ahmed Mahmood and Mandar Chitre

The authors summarize and address the problems faced during acoustic communication in snapping shrimp noise. They discuss how the noise process can be characterized by a certain statistical model based on the symmetric α-stable (SαS) family of distributions. Within the framework of this model, they highlight problems and the corresponding solutions faced in various stages of digital communication system design.

Abstract

In warm shallow waters, the ambient noise process is found to be impulsive. This phenomenon is attributed to the collective snaps created by snapping shrimp colonies inhabiting such regions. Each snap essentially creates a pressure wave, and the resulting noise process dominates the acoustic spectrum at medium-to-high frequencies. Consequently, if not addressed, *snapping shrimp noise* is severely detrimental to the performance of an *acoustic* communication system operating nearby. This article briefly summarizes and addresses the problems faced during acoustic communication in snapping shrimp noise. We discuss how the noise process can be characterized by a certain statistical model based on the symmetric α-stable (SαS) family of distributions. Within the framework of this model, we highlight problems and the corresponding solutions faced in *various stages* of digital communication system design. Both single and multicarrier systems are commented on. The resulting schemes are robust to outliers and offer excellent error performance in comparison to conventional methods in impulsive noise.

Introduction

The snapping shrimp inhabits warm shallow underwater regions around the world. These small critters live in large populations and are immediately distinguishable due to their asymmetrical front claws [1]. This physical attribute allows them to generate snaps (sudden surges in acoustic pressure) which are used for hunting prey and communicating. A typical snap, inclusive of the reverberations that follow, tends to last over a few milliseconds with peak-to-peak source levels recorded to be as high as 190 dB re 1 μPa at 1 m [1, 2]. The collective snaps of a snapping shrimp colony prove to be a challenge for underwater acoustic system designers [3]. In fact, for frequencies over 2 kHz, snapping shrimp noise is known to dominate the acoustic spectrum [4]. A noise process that depicts sudden snaps (or impulses) is rightly termed impulsive noise.

In this article, we highlight the quandary a communication system designer faces in the presence of snapping shrimp noise. We cover recent advances in the understanding of the noise process and summarize new techniques for robust digital communication in such scenarios.

Amplitude Statistics of Snapping Shrimp Noise

In Fig. 1, recorded samples of dynamic pressure for a snapping shrimp colony are presented. This data set was recorded by the Acoustic Research Laboratory (ARL) in Singapore. The snaps are clearly visible, and therefore the noise process is indeed impulsive. A first step for any communications engineer is to find a suitable model that depicts the statistics of the ambient noise process in question. In the literature, impulsive noise models are typically based on heavy-tailed distributions as they assign large probability to outliers (or extreme values). To highlight this, we present the empirical *amplitude distribution* of the noise realization in Fig. 1. We also show the fits offered by the Gaussian and symmetric α-stable (SαS) probability density functions (PDFs) under maximum-likelihood (ML) parameter estimation [5]. The well-known Gaussian PDF has light (exponential) tails and is clearly *unable* to track the empirical PDF efficiently. As observed in Fig. 1, the tails of the Gaussian curve fall rather quickly. On the other hand, the heavy-tailed SαS PDF tracks the empirical distribution fairly well. This observation is substantiated further in the literature via formal statistical tests [2, 3].

PDFs belonging to the SαS family are unimodal and symmetric (around zero). They also exhibit interesting limiting and stability properties [6]. In fact, the zero-mean Gaussian distribution is a member of the SαS family. It is well known that for a Gaussian input, the output distribution is also Gaussian under any linear transformation [7]. This result extends to SαS inputs as well and is essentially the *stability property* that is uniquely associated with this class of distributions. An SαS PDF depends on two parameters: the *characteristic exponent* $\alpha \in (0, 2]$, which controls the heaviness of the tails, and the *scale* $\delta \in \mathbb{R}^+$ [6]. Consequently, the distribution can be denoted by the abridged notation $\mathcal{S}(\alpha, \delta)$ [8]. The lower the value of α, the heavier the tails of the distribution. Moreover, for $\alpha = 2$, the SαS distribution is zero-mean Gaussian with variance $2\delta^2$, that is, $\mathcal{S}(2, \delta) \stackrel{d}{=} \mathcal{N}(0, 2\delta^2)$, where $\stackrel{d}{=}$ implies equality in distribution. With the exception of the Gaussian case, all members of the SαS family are heavy-tailed (algebraic-tailed) distributions [6]. Going back to Fig. 1, the zero-mean Gaussian and SαS fits correspond to $\mathcal{N}(0, 2(24.76)^2)$and $\mathcal{S}(1.51, 12.09)$, respectively. Note that the Gaussian distribution tries to compensate for heavier tails by increasing the scale.

Digital Object Identifier:
10.1109/MCOM.2017.1500617

The authors are with the National University of Singapore.

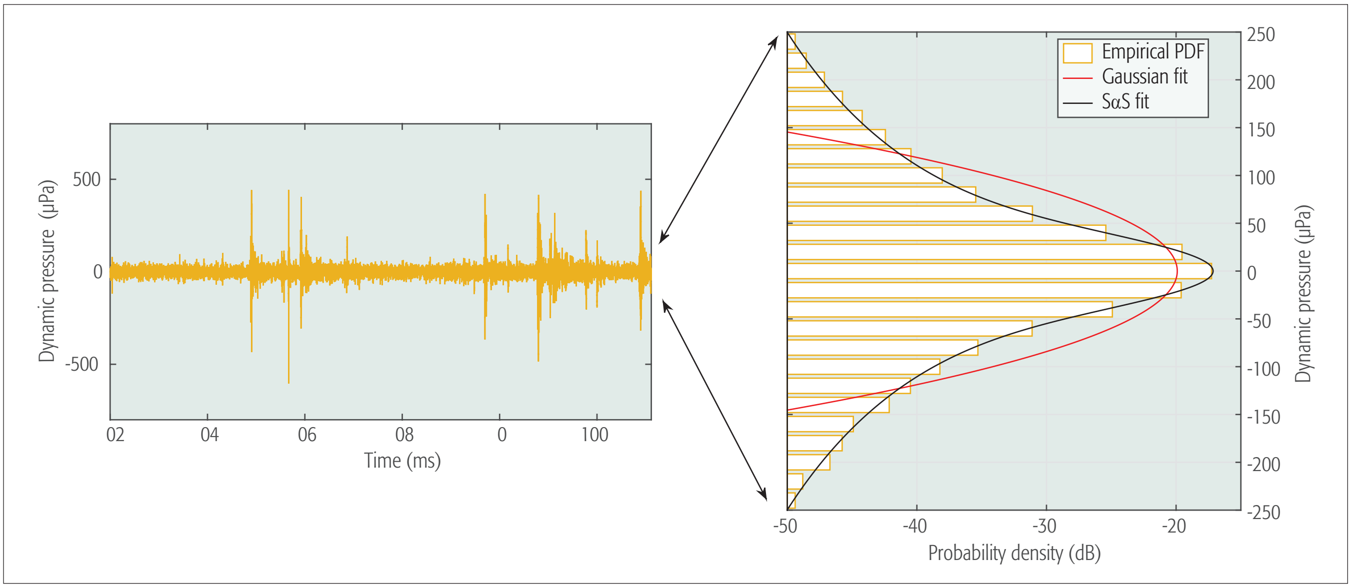

Figure 1. An uncoded receiver schematic.

As the SαS PDF offers a good fit to the empirical amplitude distribution in Fig. 1, the communication techniques we highlight later on are tuned to combat non-Gaussian white SαS noise (WSαSN). For α = 2, the WSαSN is a white Gaussian noise (WGN) process. Though "white" implies a flat power spectral density (PSD) for the latter case, this definition does not extend to non-Gaussian SαS models as the underlying distributions have *infinite* second order moments [6]. We reserve the term to highlight the fact that samples of the noise process are independent and identically distributed (IID) SαS random variables.

Passband and Baseband Communication

In an underwater acoustic system, frequency-dependent path loss and non-uniform ambient noise spectra restrict conducive transmission to a band-limited spectrum [9]. Moreover, if communication is required over larger distances, additional limitations are put on the bandwidth. Therefore, to harness the "good" characteristics of the channel, signal transmission is performed in the passband. Consequently, ambient noise encountered in underwater scenarios (and hence WSαSN) is an *additive passband* noise process. As a first step, classical texts and techniques rightly convert the received signal to its baseband form to do away with the carrier component that inherently accompanies the passband signal [7]. By doing so, subsequent processing can be performed at relatively low rates (i.e., comparable to the transmission rate). This is why most papers start off by introducing baseband signals and models and not their passband counterparts. Therefore, understanding the baseband statistics of a passband non-Gaussian WSαSN process is essential for communication system design in warm shallow waters.

In a typical digital communications scheme, information is represented as a sequence of symbols. The total number of possible symbols is finite, and each symbol can be represented mathematically by a point on the complex plane [7]. The collective set of these points is a *constellation*, and we denote it by $\mathcal{X}$. For transmission, a chosen symbol $x \in \mathcal{X}$ is initially multiplied onto a real low-frequency band-limited waveform $g(t)$ to create the baseband signal. This is subsequently multiplied by a high-frequency carrier wave to generate the passband signal. The relationship between these signals is represented by perhaps the most well-known expression in digital communications, $s(t) = \Re\{xg(t)e^{j2\pi f_c t}\}$, where $s(t)$ is the passband signal, f_c is the carrier frequency, and $\Re\{\cdot\}$ is the real operator [7]. In a noise-only scenario, the receiver's objective is to retrieve the transmitted symbol from $r(t) = s(t) + w(t)$, where $w(t)$ is the additive noise process. Conventionally, this is achieved by processing $r(t)$ to get $b(t) = h(t)*r(t)e^{-j2\pi f_c t}\}$. Here $h(t)$ is the impulse response of a lowpass filter with bandwidth equal to that of $g(t)$, and $*$ is the *linear convolution* operator. The signal $b(t)$ is subsequently passed through a filter matched to $g(t)$, which results in the simplified form $r = x + w$, where $r, w \in \mathbb{C}$ are the received (noisy) symbol and additive noise component, respectively [7]. We refer to this entire process as *conventional* baseband conversion and note that it is a linear system. Finally, the received observations r are mapped onto the most probable symbol $\hat{x}$ in the constellation via a detection rule.

A general block diagram of an uncoded digital communication receiver is presented in Fig. 2. For a given *passband* noise process, the *baseband statistics* are determined by the mechanism adopted for baseband conversion. If one understands these statistics, the pattern of received (noisy) observations on the corresponding scatter plot can easily be discerned. This in turn will influence the design of the employed constellation and detection scheme. In the subsequent text, we offer insights and good design guidelines for the steps labeled in Fig. 2 for robust communication in snapping shrimp noise.

Remark: In this article, we address only the problem of communication in ambient noise and *do not* consider the underwater acoustic channel. Estimating and equalizing the channel in snapping shrimp noise is an independent problem [8, 10]. Second, this article highlights how to improve

If communication is required over larger distances, additional limitations are put on the bandwidth. Therefore, to harness the "good" characteristics of the channel, signal transmission is performed in the passband. Consequently, ambient noise encountered in underwater scenarios (and hence WSaSN) is an additive passband noise process.

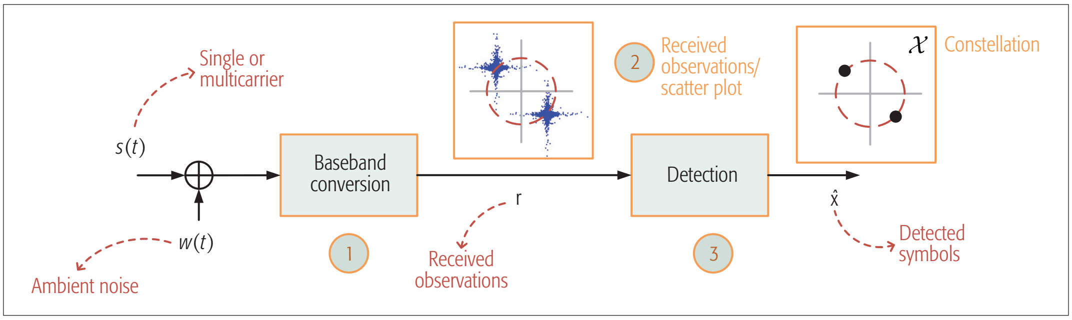

Figure 2. An uncoded receiver schematic.

performance of an *uncoded* communication scheme in impulsive noise. Although error correcting codes do enhance the robustness of the system, this comes with increased computational complexity [7]. As seen in the subsequent text, even for an uncoded system, the complexity of the *optimal* receiver is high.

On Introducing Passband Sampling

In a typical communications receiver, the baseband conversion block is implemented via *linear analog filters* [7]. However, depending on the range, physical constraints limit f_c and the bandwidth in underwater acoustic transmission to a few tens/hundreds of kilohertz [9]. Therefore, due to its low Nyquist rate, one may easily *sample* the passband signal before conversion to baseband form. Doing so would also require discretizing operations within the baseband conversion block in Fig. 2. More precisely, on introducing *uniform* sampling, $r[n] = s[n] + w[n]$ and

$$b[n] = \frac{1}{f_s} h[n] * r[n] e^{-j2\pi f_c/f_s n}, \tag{1}$$

where f_s is the passband sampling frequency, n is the discrete-time index, and square brackets denote discrete signals obtained by sampling their continuous-time counterparts at $t = n/f_s \in n \in \mathbb{Z}$. Finally, $b[n]$ is passed through a filter matched to $g[n]/f_s$ to get $r = x + w$.

Let W denote the complex random variable with outcome W. For WGN and *conventional* baseband conversion, it is well known that W follows a zero-mean isotropic bivariate Gaussian distribution [7]. Introducing *uniform* passband sampling and discretizing the subsequent operations does not alter its baseband form [8]. However, if WGN is replaced by non-Gaussian WSαSN, one can actually *vary* the statistics of W by tweaking f_s with respect to f_c. The corresponding baseband noise PDFs will always be *bivariate* SαS due to the stability property associated with them and the linearity of the receiver [8]. However, they may be remarkably *dissimilar* for different f_s and f_c. We show three such instances in Fig. 3. For this example, we consider a WSαSN process with $\alpha = 1.5$ as this signifies typical estimates in *severe* snapping shrimp noise [2, 3]. As all non-Gaussian SαS distributions are heavy-tailed, the geometries of the PDFs in Fig. 3 extend to all other values of α, with the exception of $\alpha = 2$ [8].

On inspection, one can see that the PDFs in Fig. 3 have protruding "tails" in specific directions. This is more apparent in the top views of the PDFs, also shown in Fig. 3. Mathematically, the number of tails is determined by

$$N_T = \begin{cases} \dfrac{f_s}{\gcd(f_c, f_s)} & \text{if } f_s \text{ is an even multiple of } f_c \\ \dfrac{2f_s}{\gcd(f_c, f_s)} & \text{o.w,} \end{cases} \tag{2}$$

where $\gcd(f_c, f_s)$ is the greatest common divisor of f_c and f_s [11]. Due to uniform sampling and independent passband noise samples, the tails are located *uniformly* around the origin [8]. Consequently, from Eq. 2, the angle between adjacent tails is $\psi_T = 2\pi/N_T$ radians. Furthermore, the isotropic PDF can be interpreted as having an infinite number of tails and is the limiting case $f_s \to \infty$ (i.e., no passband sampling) [8]. So what do these tail structures imply? Impulses encountered in the *passband* WSαSN process are directed along these tails upon *baseband* conversion with *large probability*. For example, for the four-tailed PDF in Fig. 3, a passband snap will *most probably* end up lying in one of four possible directions in the complex plane (i.e., along either coordinate axis). Similarly, the six-tailed PDF tells us that an impulse lies in any one of only six directions with high probability. Therefore, by merely employing *uniform* passband sampling and tuning f_c and f_s, one can control the placement of outliers in a probabilistic sense via N_T (or ψ_T) in the complex plane.

It is not hard to see why a PDF with *smaller* N_T offers *more* information about an impulse. For example, in Fig. 3, the isotropic PDF offers *no insight* on the location of an impulse in the complex plane. It could lie anywhere on a circle centered at the origin with equal probability. On the contrary, the four-tailed PDF should offer the *most* information among the displayed PDFs as outliers most probably occur along the positive and negative directions of each axis. Thus, for smaller N_T, impulses are more *localized* (in a probabilistic sense) in the complex plane, and there is *less* ambiguity associated with them [8]. On another note, if one samples the WSαSN process above the Nyquist rate of $s(t)$, it turns out that $N_T = 4$ is the *minimum* number of tails that can be generated for W. This in turn is *only possible* when $f_s = 4f_c$ and results in the four-tailed PDF in Fig. 3 [8, 12]. Using these insights, one may design better communication schemes by exploiting the localized impulse information offered by the four-tailed baseband noise PDF at the *detection stage*.

Denoting the real and imaginary components of W as W_R and W_I, respectively, the four-tailed PDF arising from the $f_s = 4f_c$ constraint has another desirable characteristic: W_R and W_I are IID non-Gaussian SαS random variables [11]. This is observed from Eq. 1, where $e^{-j2\pi f_c/f_s n}$ simplifies to

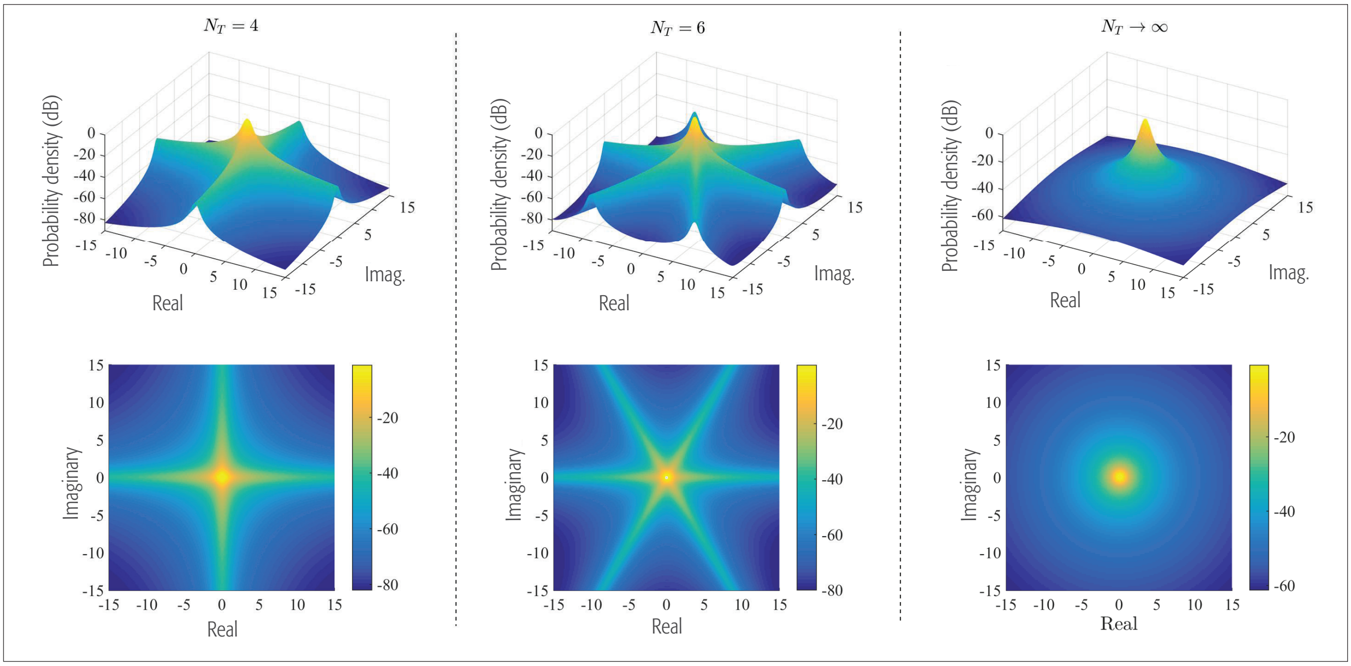

Figure 3. Instances of baseband noise PDFs of passband WSαSN with α = 1.5. From left to right: A four-tailed PDF, a six-tailed PDF, and an isotropic PDF. The bottom row offers top views of the bivariate PDFs.

$e^{-j\pi n/2} \in \{\pm 1, \pm j\}$. Note that the latter outputs purely real or imaginary values for evenly and oddly indexed samples of $w[n]$, respectively. Consequently, W_R and W_I are constructed from non-overlapping WSαSN samples and are thus independent. Moreover, all passband WSαSN samples are processed by the same baseband conversion block. Therefore, W_R and W_I are identical [12].

On another note, the $f_s = 4f_c$ constraint also results in the *best possible* baseband conversion scheme for a *linear* system operating in passband WSαSN and can be explained by an entropy argument [12]. The *joint-entropy* $H(W_R, W_I)$ of W_R and W_I can be expressed as

$$H(W_R, W_I) = H(W_R) + H(W_I) - I(W_R; W_I), \quad (3)$$

where $H(W_R)$ and $H(W_I)$ are the *self-entropies* of W_R and W_I, respectively, and $I(W_R; W_I)$ is the *mutual information* between them. We note that $H(W_R, W_I)$ is constant for a given $b[n]$ and $H[n]$. Moreover, $I(W_R; W_I)$ depends on the joint-PDF of W_R and W_I, and thus varies for different f_c. Consequently, as $I(W_R; W_I)$ increases, $H(W_R)$ and $H(W_I)$ increase accordingly to satisfy Eq. 3. One notes that if W_R and W_I are independent, $I(W_R; W_I) = 0$, and $H(W_R)$ and $H(W_I)$ are at their respective minimums. Due to the linearity of the receiver, baseband conversion can be *equivalently* represented by two parallel blocks that *individually* process the in-phase and quadrature components of $r[n]$ [7]. Thus, the receiver is unable to exploit the dependency between W_R and W_I, which is why it performs at its best when $I(W_R; W_I) = 0$ (i.e., when W_R and W_I are independent). The latter holds true if and only if $f_s = 4f_c$.

The above discussion highlights why the $f_s = 4f_c$ constraint is desirable for linear baseband conversion. Moreover, the associated four-tailed PDF offers a further advantage at the detection stage. We therefore use this configuration to design the constellation and detector labeled in Fig. 2.

A Study Case: BPSK

Now that we know what characteristics are best suited for W, the next step is to devise mechanisms that exploit the corresponding noise information. We do this for a single-carrier binary phase shift keying (BPSK) scheme. In Fig. 4 we highlight two BPSK constellations,

$$\chi_1 \in \{\pm 1\} \text{ and } \chi_2 \in \left\{\pm\sqrt{1/2}(1-j)\right\},$$

and note that they are merely *rotated* versions of each other. Also shown are the corresponding scatter plots based on the four-tailed baseband noise PDF. By just rotating $\mathcal{X}_1$, we are able to generate the symbol map $\mathcal{X}_2$ where the tails in the scatter plot are directed *away* from the opposing symbol in the constellation. This is an important aspect of design. Intuitively, if the tails corresponding to one symbol interfere with those of the other, the detector is unable to recover most of the transmitted symbols from observations that fall in these overlapping regions. Moreover, as tail observations occur with non-negligible probability, system error performance degrades sharply. From this argument, we see that $\mathcal{X}_1$ is a sub-optimal constellation, while $\mathcal{X}_2$ offers minimum overlap between the corresponding tails [8].

For the system to be truly robust in impulsive noise, a suitable detection scheme has to be invoked in conjunction with the optimized BPSK constellation $\mathcal{X}_2$. Intuitively, from Fig. 4, one observes that a good detector should map observations *lying along* the tails to the associated transmitted symbol as they occur with *high* probability. The ML detector does this optimally, but it needs to numerically evaluate the SαS PDF every time it makes a decision as the latter cannot be expressed in closed form. This could potentially be too taxing for real-time systems that need to

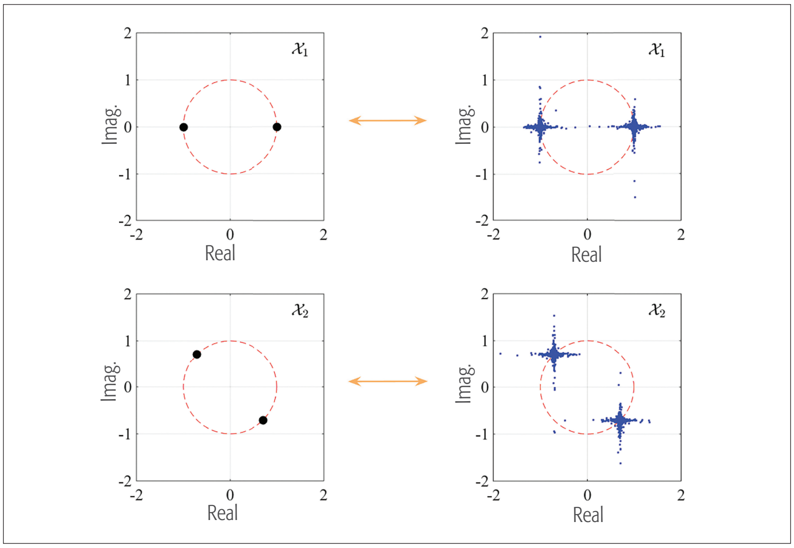

Figure 4. BPSK constellations and scatter plots.

operate at certain data rates. To avoid this, one may look toward generalized ML (or M-estimation) theory [13]. Mathematically, the ML detector has the form $\hat{x}$ = argmax $f_W(r - \mu)$ w.r.t. $\mu \in \mathcal{X}$, where $f_W(\cdot)$ is the bivariate PDF of W. As W_R and W_I are IID SαS random variables, we have $f_W(w) = f(w_R)f(w_I)$ where W_R and W_I are the real and imaginary components of W, respectively, and $f(\cdot)$ is the univariate SαS PDF of W_R and W_I. From M-estimation theory, one can replace $f(\cdot)$ by an arbitrary function $\rho(\cdot) \in \mathbb{R}^+$. To achieve near-optimal performance, $\rho(\cdot)$ should *approximate* $f(\cdot)$ as close as possible. Robust functions such as the L_p-norm (for $0 \le p < 2$) and the myriad are able to do just that while simultaneously offering closed-form expressions for $\rho(\cdot)$ [8, 12].

The error performance of a digital communication system is typically measured against the signal-to-noise ratio (SNR) per bit E_b/N_0, where E_b is the bit energy and $N_0/2$ is the two-sided PSD of the white noise process [7]. As the PSD of non-Gaussian WSαSN is infinite, N_0 does not carry the same meaning here. However, it can be represented in terms of the *scale parameter* of the *passband* noise samples [8, 12]. More precisely, as $W[n]$ are samples of WSαSN, each sample is an $\mathcal{S}(\alpha, \delta)$ distributed random variable. Using the fact that $\mathcal{S}(2, \delta) \overset{d}{=} \mathcal{N}(0, 2\delta^2)$ and $N_0 f_s/2$ is the variance of a WGN process with PSD $N_0/2$, we have $N_0 = 4\delta^2/f_s$. We thus employ $E_b f_s/4\delta^2$ as our SNR measure.

We present the bit error rate (BER) performance of $\mathcal{X}_2$ with the myriad detector in Fig. 5 (solid blue line) in the presence of WSαSN for α = 1.5. This value of α adequately models the empirical density function of severe snapping shrimp noise [2]. For comparison, we also present the BER of the same system but with $\mathcal{X}_1$ (blue dotted line). Moreover, to see how the noise PDF influences system performance, we plot the BER corresponding to the case of *no passband* sampling (red dotted line). As this setup results in W having an isotropic PDF, rotating the BPSK constellation offers no additional advantage in terms of BER. We also employ the Euclidean detector in this scenario as it is optimal for isotropic PDFs [7]. Clearly, the performance gain of the system employing $f_s = 4f_c$, $\mathcal{X}_2$ and the myriad detector (solid blue line) over all other schemes is substantial. At a BER of 10^{-4}, the gain is approximately 13 dB.

From an implementation perspective, one can arbitrarily rotate a constellation *at the receiver* by sampling $r(t)$ with a phase offset [8]. Consequently, the transmitter does not need to know the optimal rotation of the constellation. Moreover, this also allows nullifying any random rotation (if known) introduced by the channel. Thus, for BPSK, one may transmit symbols from $\mathcal{X}_1$ but still achieve the BER performance corresponding to $\mathcal{X}_2$ by sampling $r(t)$ appropriately at the receiver.

Nonlinear Baseband Conversion

Until now we have discussed how a *linear* receiver can be optimized in the presence of non-Gaussian WSαSN. This was accomplished by employing passband sampling at $f_s = 4f_c$, suitable constellations, and robust detectors. However, *linear systems* are known to be sub-optimal in impulsive noise [12, 13]. Indeed, the previous discussion only introduces robust measures at the detection stage, not during baseband conversion. By removing the linear constraint and using suitable nonlinear baseband conversion mechanisms, the BER performance of the communications system can be enhanced *substantially* further. Not only does this enhance robustness, but it also reduces the loss in E_b/N_0 due to the inefficiency of linear systems in impulsive noise [8, 12].

The baseband conversion block in Fig. 2 maps the received passband samples $r[n]$ onto the observation r. This mapping is essentially a solution for an estimation problem whose parameter space is the complex plane. The ML estimator offers the optimal solution and is *nonlinear* for WSαSN [8]. Mathematically, this is given by

$$r = \mathtt{argmax} \prod_{n=0}^{K-1} \tilde{f}\left(r[n] - \Re\left[\left\{\mu b[n] e^{j\pi n/2}\right\}\right]\right)$$

w.r.t $\mu \in \mathbb{C}$, where K is the number of samples per transmitted symbol and $\tilde{f}(\cdot)$ is the PDF of a sample of WSαSN. For a given E_b/N_0, the performance of the ML estimator increases *monotonically* with K, or in other words, the ratio of available bandwidth to transmission bandwidth [12]. To understand why, from Fourier transform theory, we note that the energy of an impulse is distributed over the entire spectrum. Therefore, *all* frequency bands contain some information about the impulse. Correspondingly, due to numerous outliers in WSαSN, noise components in non-overlapping frequency bands are *dependent*. As a noise process is deemed impulsive *relative to* the transmitted signal, by considering a larger bandwidth than the latter, a receiver can potentially exploit the out-of-band information to reduce the in-band noise [8, 12].

With a few added considerations, the error performance of a communications scheme employing ML baseband conversion can surpass that of an optimized linear system [12]. To highlight this, we also plot the attainable BER of such a scheme in Fig. 5 (red dash-dot line). Clearly, the resulting system is much more robust to snaps than all other presented schemes and offers approximately 16 dB gain over the best linear receiver at a BER of 10^{-4}. One disadvantage of using ML baseband conversion is the computational complexity that is implicitly associated with it. The cost function itself is not in closed-form and needs to be solved numerically at rates comparable to f_s [8]. However, similar to our discussion on robust detectors, one can revert to M-estimation theory and substitute $\tilde{f}(\cdot)$ by some closed-form function $\rho(\cdot) \in \mathbb{R}^+$ [13]. The L_p-norm (for $0 \leq p < 2$) and myriad offer suitable substitutes for $\rho(\cdot)$ and offer near-optimal error performance. Further still, as L_p-norm minimization for $1 \leq p < 2$ is a convex problem, efficient solvers do exist that are implementable in real-time systems [8].

Multicarrier Communication

Until now, we have discussed how a *single-carrier* BPSK scheme can be optimized to enhance system error performance in snapping shrimp noise. If one employs a multicarrier scheme, such as orthogonal frequency-division multiplexing (OFDM), would there be any added advantage? The answer is yes. From the discussion in the previous section, we already know that information of an impulsive noise process is spread out over a bandwidth larger than the signal bandwidth. In an N-carrier OFDM system, the signal bandwidth is further divided into N sub-bands. Therefore, the ratio of the available bandwidth to that of a sub-band is N times larger than that of a single-carrier system operating in the same band. Consequently, the noise information *per transmitted symbol* is higher in the former case and can be used to enhance the error performance of the system. In fact, as N increases, the error performance of the system can be made *increasingly* better due to the consistently smaller bandwidths allocated to each sub-band. The added information per symbol is harnessed at the detection stage, which is performed jointly across all carriers [14]. Like the single-carrier case, the detector may be based on the ML, the L_p-norm, or the myriad detector. As an added bonus, the per-carrier baseband noise PDF and constellation cease to influence the error performance of the system for large N [14]. In Fig. 6, we plot the BER of an OFDM system employing optimally rotated BPSK constellations and ML detection for various N in WSαSN with $\alpha = 1.5$. For these results, we assume the baseband noise statistics follow the four-tailed PDF in Fig. 3 This is obtained by using $f_s = 4f_c$ and *linear* baseband conversion.

On the downside, the computational complexity of the optimal (ML) detector for an N-carrier OFDM system in non-Gaussian WSαSN is high [8, 14]. If BPSK is the employed constellation, the detector's complexity is $O(2^M)$, where $0 < M \leq N$ is the number of data carriers. To exploit the advantages offered by an OFDM scheme, M and N are typically set to be large numbers. Even for a moderate number of carriers, such as $N = 32$ or $N = 64$, the number of computations required for optimal detection is substantial. However, in [8, 14], near-optimal performance is achieved by using detectors that operate in linear time. The proposed schemes approximate the combinatorial detection problem by a convex problem whose parameter space is of dimension $2M$. Thereafter, separate detectors are applied on each carrier. The runtime is further reduced by using tools such as compressed sensing to reduce the dimensionality of the problem to $2(N - M)$ [14].

Like the single-carrier case, one may use a nonlinear baseband conversion scheme to further enhance performance of the OFDM system [14]. This offers more robustness to the noise samples by using a larger bandwidth (due to the higher f_s) and nullifies the loss in E_b/N_0 that is inherent for linear systems in impulsive noise [8, 14].

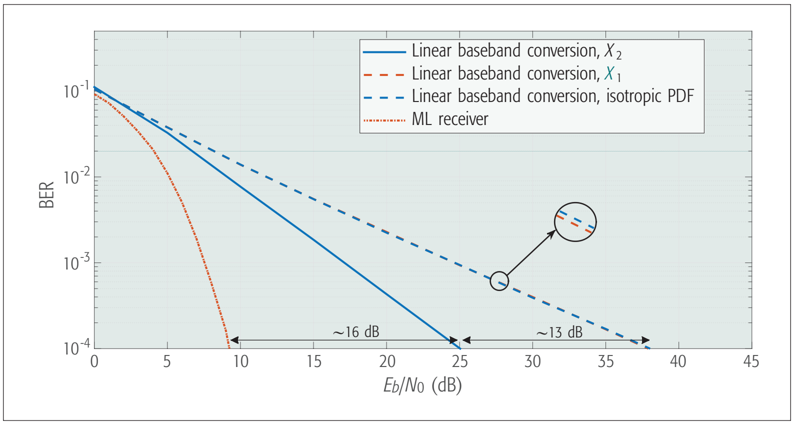

Figure 5. Single-carrier BPSK BER performance for various receivers in WSSN for α = 1.5.

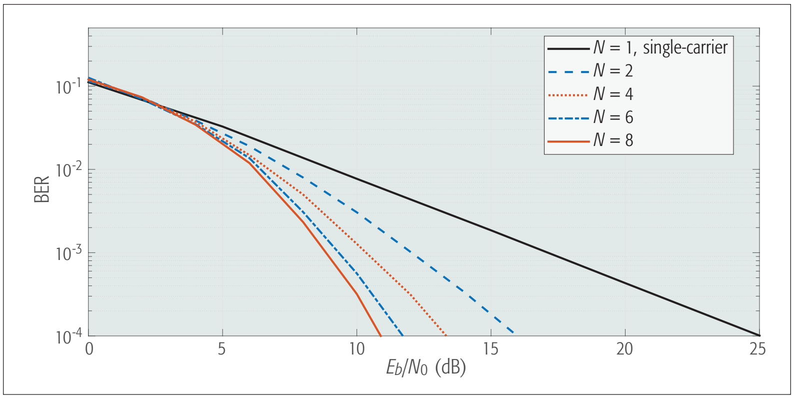

Figure 6. ML detection performance of BPSK-OFDM with varying N in WSaSN for α = 1.5.

Conclusion

This article provides a brief outlook on the problems faced by communication engineers in underwater scenarios dominated by snapping shrimp noise. Design guidelines that allow robust communication in such scenarios are visited. A summary is provided as follows:

- The amplitude statistics of snapping shrimp noise is modeled well by heavy-tailed SαS PDFs.
- The baseband noise statistics for a non-Gaussian passband WSαSN process is analyzed. The PDFs are symmetric and heavy-tailed, and take star-shaped configurations in the complex plane.
- Of all possible baseband noise PDFs, the one with the minimum number of tails offers the most information about the location of impulses in the complex plane. If the Nyquist sampling criterion of the transmitted signal is fulfilled, the minimum number of tails is four.
- Using this information, constellations can be designed in such a way as to avoid interference between received observations of different symbols.
- In conjunction with the good constellations, robust detectors need to be invoked to enhance the error performance of the communications system. A good detector exploits the tailed structure

Multicarrier schemes, such as OFDM, can take advantage of the larger noise information per transmitted symbol to offer better error performance than their single-carrier counterparts. This can be done by performing detection jointly among the carriers.

of the baseband noise PDF and maps observations lying along these tails accordingly.

•Linear systems are sub-optimal in impulsive noise. Therefore, conventional baseband conversion may be replaced by suitable nonlinear mechanisms to enhance the error performance even further. Near-optimal receivers exist that process in linear time, thus allowing real-time implementability.

•Multicarrier schemes, such as OFDM, can take advantage of the larger noise information per transmitted symbol to offer better error performance than their single-carrier counterparts. This can be done by performing detection jointly among the carriers. Additionally, the baseband noise PDF and constellations cease to influence the error performance of the system when the number of carriers is large.

•The combinatorial joint detection problem in OFDM is approximated well by certain convex problems. These offer near-optimal solutions that may be generated in real time.

In retrospect, one notes that the aforementioned schemes are robust to outliers in snapping shrimp noise. However, in Fig. 1, we see that the realization, besides being impulsive, is bursty as well (i.e., the impulses cluster together). If the dependency between samples is taken into account, the performance of communication schemes may be pushed even further. To do this, appropriate temporal models need to be derived [2]. Current research trends are shifting toward developing more rigorous models to depict the memory of the snapping shrimp noise process. In particular, [15] uses a sliding window type framework that not only ensures each sample to be SαS, but also models the dependency between them. Developing optimized communication schemes for such models offers a promising prospect for future acoustic systems operating in warm shallow waters.

References

[1] W. W. L. Au and K. Banks, "The Acoustics of the Snapping Shrimp Synalpheus Parneomeris in Kaneohe Bay," *J. of the Acoustical Soc. of Amer.*, vol. 103, no. 1, 1998, pp. 41–47.

[2] M. W. Legg, *Non-Gaussian and Non-Homogeneous Poisson Models of Snapping Shrimp Noise*, Ph.D. dissertation, Curtin Univ. of Technology, 2009.

[3] M. Chitre, J. Potter, and S.-H. Ong, "Optimal and Near-Optimal Signal Detection in Snapping Shrimp Dominated Ambient Noise," *IEEE J. Ocean. Eng.*, vol. 31, no. 2, Apr. 2006, pp. 497–503.

[4] J. R. Potter, T. W. Lim, and M. A. Chitre, "Ambient Noise Environments in Shallow Tropical Seas and the Implications for Acoustic Sensing," *Oceanology Int'l.*, vol. 97, 1997, pp. 2114–17.

[5] J. Nolan, "Maximum Likelihood Estimation and Diagnostics for Stable Distributions," *Lévy Processes*, O. Barndorff-Nielsen, S. Resnick, and T. Mikosch, Eds., Birkhuser, 2001, pp. 379–400; http://dx.doi.org/10.1007/978-1-4612-0197-7 17.

[6] J. P. Nolan, *Stable Distributions — Models for Heavy Tailed Data*. Birkhauser, 2015, Ch. 1; http://fs2.american.edu/jpnolan/www/stable/stable.html.

[7] J. Proakis and M. Salehi, *Digital Communications*, ser. McGraw-Hill Higher Education, McGraw-Hill Education, 2007.

[8] A. Mahmood, *Digital Communications in Additive White Symmetric Alpha-Stable Noise*, Ph.D. dissertation, Nat'l. Univ. of Singapore, June 2014.

[9] M. Stojanovic and J. Preisig, "Underwater Acoustic Communication Channels: Propagation Models and Statistical Characterization," *IEEE Commun. Mag.*, vol. 47, no. 1, Jan. 2009, pp. 84–89.

[10] K. Pelekanakis and M. Chitre, "Adaptive Sparse Channel Estimation under Symmetric Alpha-Stable Noise," *IEEE Trans. Wireless Commun.*, vol. 13, no. 6, June 2014, pp. 3183–95.

[11] A. Mahmood, M. Chitre, and M. A. Armand, "PSK Communication with Passband Additive Symmetric-Stable Noise," *IEEE Trans. Commun.*, vol. 60, no. 10, Oct. 2012, pp. 2990–3000.

[12] —, "On Single-Carrier Communication in Additive White Symmetric Alpha-Stable Noise," *IEEE Trans. Commun.*, vol. 62, no. 10, Oct. 2014, pp. 3584–99.

[13] P. Huber and E. Ronchetti, *Robust Statistics*, ser. Wiley Series in Probability and Statistics, Wiley, 2009.

[14] A. Mahmood, M. Chitre, and M. A. Armand, "Detecting OFDM Signals in Alpha-Stable Noise," *IEEE Trans. Commun.*, vol. 62, no. 10, Oct. 2014, pp. 3571–83.

[15] A. Mahmood and M. Chitre, "Modeling Colored Impulsive Noise by Markov Chains and Alpha-Stable Processes," *MTS/IEEE Oceans — Genoa*, May 2015, pp. 1–7.

Biographies

Ahmed Mahmood [S'11, M'14] received his B.Eng and M.Eng degrees in electrical engineering from the National University of Sciences and Technology (NUST), Pakistan, and a Ph.D. degree from the Department of Electrical & Computer Engineering, National University of Singapore (NUS). In 2014, he joined the Acoustic Research Laboratory (ARL) at NUS, where he is now a research fellow. His current research interests involve underwater acoustic communications, robust signal processing, channel modeling, estimation and detection theory, and error correction coding for impulsive noise. He has served as a reviewer for several technical journals, including *IEEE Transactions on Communications*, *IEEE Transactions on Signal Processing*, the *IEEE Journal of Oceanic Engineering*, *IEEE Communications Letters*, and *IEEE Signal Processing Letters*. He was the TPC Chair for WUWNet '16.

Mandar Chitre [S'04, M'05, SM'11] received B.Eng. and M.Eng. degrees in electrical engineering from NUS in 1997 and 2000, respectively, an M.Sc. degree in bioinformatics from Nanyang Technological University (NTU), Singapore, in 2004, and a Ph.D. degree from NUSin 2006. From 1997 to 1998, he worked with the ARL, NUS. From 1998 to 2002, he headed the technology division of a regional telecommunications solutions company. In 2003, he rejoined ARL, initially as the deputy head (research) and now head of the laboratory. He also holds a joint appointment with the Department of Electrical and Computer Engineering at NUS as an associate professor. His current research interests are underwater communications, underwater acoustic signal processing, and marine robotics. He has served on the Technical Program Committees of IEEE OCEANS, WUWNet, DTA, and OTC, and has served as a reviewer for numerous international journals. He was the Chairman of the Student Poster Committee for IEEE OCEANS '06 in Singapore, the Chairman of the IEEE Singapore AUV Challenge 2013, and the TPC chair for the WUWNet conference. He is currently Co-Chair of the IEEE Ocean Engineering Society Technology Committee on Underwater Communication, Navigation and Positioning.